PHYSICAL REVIEW B **74**, 184208 (2006)

Rigidity and intermediate phases in glasses driven by speciation

Matthieu Micoulaut
Laboratoire de Physique Théorique de la Matière Condensée, Université Pierre et Marie Curie, UMR 7600 CNRS,
Boite 121, 4, Place Jussieu, 75252 Paris Cedex 05, France
(Received 17 October 2006; published 30 November 2006)

Rigidity transitions that separate elastic phases in glasses are studied in the case where the local structure is not fully determined from the macroscopic concentration. It is shown that the location of the rigidity transitions, and the intermediate phase that separates flexible from stressed rigid glasses, depend crucially on the way local structures are selected, a selection usually termed speciation. Broadening of the intermediate phase is obtained for networks combining a large amount of flexible local structural units and extensive medium range order. This applies to systems of the form $(1-x)\mathrm{Si}X_2-xM_2X$ (X=O, S, Se, M=Li, Na, K) and opens additional perspectives for the observation of self-organized fast ionic conductors or geomaterials.

DOI: 10.1103/PhysRevB.74.184208 PACS number(s): 61.43.Fs, 83.80.Ab

I. INTRODUCTION

A variety of different physical behaviors can be observed in structural glasses that are related to the connectedness of their backbones. On a microscopic level, nearest-neighbor bonding interactions between atoms (bond bending and bond stretching) can be visualized as Lagrangian mechanical constraints[1] to predict the elastic behavior of glassy networks. The enumeration n_c of these constraints per atom, when compared to the number of degrees of freedom, defines then underconstrained (flexible) or overconstrained (stressed rigid) glasses. A vibrational analysis[2] shows that these flexible and stressed rigid glasses are separated by an elastic phase transition when the network mean coordination number $\bar{r}$ reaches the critical value $\bar{r}_c=2.38$. In stressed rigid networks ($\bar{r}>\bar{r}_c$), the number of zero-frequency (floppy) vibrational modes (which acts as the order parameter of the transition) goes to zero and the elastic constants display a power-law behavior with $\bar{r}$. At the transition, glassy networks are optimally constrained (isostatically rigid, $n_c=3$).[1]

The underlying nature of this peculiar transition has been reinvestigated recently because two transitions at different mean coordination numbers $\bar{r}_{c(1)}$ and $\bar{r}_{c(2)}$ have been found[3] experimentally in a certain number of glasses. These define an *intermediate phase* (IP) between the flexible and the stressed rigid phases where glasses display some remarkable properties such as absence of aging[4] or stress,[5] or selection of isostatically rigid local structures.[3] The two boundaries of the IP have been characterized from numerical calculations,[6,7] cluster analysis,[8] and energy adaptation[9] on self-organized networks and identified as being a rigidity transition at low $\bar{r}$ and a stress transition at high $\bar{r}$. In the mean-field approach or in random networks both transitions coalesce into a single one. In network glasses, the short-range order and the mean coordination number are imposed by the macroscopic concentration of the atoms involved (e.g., $\bar{r}=2+2x$ in the archetypal $\mathrm{Ge}_x\mathrm{Se}_{1-x}$).[3,4] In this case, self-organization is achieved through the nucleation of weakly stressed rigid medium-range-order elements such as small rings[6] that delay the onset of stressed rigidity.

Links between the IP and protein folding,[10] high-temperature superconductors,[11] or computational phase transitions[12] have been stressed that go much beyond simple analogies. The understanding of the IP in glasses where the structure can be steadily changed with composition is therefore of general interest.

If now the macroscopic concentration does not fully define the short-range-order elements, can new local structural degrees of freedom contribute to stress avoidance of the network? And in what manner? Here it is shown how the selection of more flexible local structural units shifts the stress transition to higher $\bar{r}$, and leads to the broadening of the IP, independently of the degree of medium-range order. The latter contributes, however, to the increase of $\Delta\bar{r}=\bar{r}_{c(2)}-\bar{r}_{c(1)}$ as well. On the other hand, the possibility of the system to select local structures in order to lower the constraint free energy in the stressed rigid phase leads to a situation that resembles very much the sodium silicates. Taken together, these results provide benchmarks to study IP's in multicomponent glass systems such as geomaterials or fast ionic conductors where the elastic nature of the network crucially determines physical and electric or mass transport properties.

The recent discovery of an IP in silicates[13] illustrates this challenging issue. Spectroscopic studies have indeed shown that, e.g., lithium silicate glasses (with network former SiO_2 and network modifier $\mathrm{Li_2O}$) are made of several lithium silicate species, distinguished by their number of bridging oxygen atoms.[14] Thus the local structures (or species) present at low modifier concentration are $\mathrm{SiO}_{4/2}$ (the tetrahedron that forms silica), $\mathrm{LiSiO}_{5/2}$, and $\mathrm{Li_2SiO}_{6/2}$ usually named as Q^4, Q^3, and Q^2 "species," respectively (Fig. 1). For each Q^n, n is the number of bridging oxygen atoms that connect silicon tetrahedra to the rest of the network. The relative abundance of these local structures and the way they behave with the modifier concentration (or temperature, or pressure in geological studies) is usually termed[14,15] as *speciation*. The fact that the variation of the relative abundance of the species with composition is not trivial now contributes to $\bar{r}$ in a nonlinear fashion. A simple model to highlight the effect of the speciation is solved, and combined with cluster-constraint calculations applied to silicate or thiosilicates of the form $(1-x)\mathrm{Si}X_2-xM_2X$ with X=O, S, Se and M=Li, Na, K which are optimally constrained ($n_c=3$) at $x=0.20$.[16]

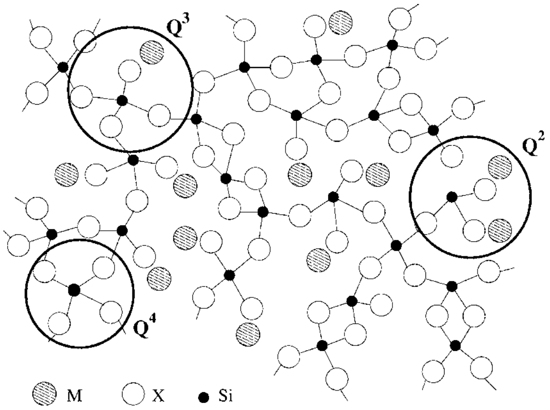

FIG. 1. Example of a network of $(1-x)\mathrm{Si}X_2-xM_2X$ with three kinds of species (Q^2, Q^3, and Q^4, defined in the marked circles).

In binary sodium silicates (X=O, M=Na), speciation (i.e., the Q^n distribution with x) is very simple because the modifier cation M creates almost only Q^3 units at low x so that the probability of finding the latter is $R=2x/(1-x)$. This means that the disproportionation reaction[17]

$$2Q^3 \rightleftharpoons Q^4 + Q^2 \tag{1}$$

involving the species Q^n is shifted to the left side. Equation (1) can be considered as an equilibrium reaction with an equilibrium constant defined from the probabilities of finding the different species:

$$K_e = \frac{p_4^{(1)} p_2^{(1)}}{p_3^{(1)} p_3^{(1)}} \tag{2}$$

since (i) NMR supports[18] the existence of a limited number of chemical species in the glass and the melt and (ii) ln K_e is linear with $1/T$ (van't Hoff's equation) and has a reaction enthalpy that is correlated[19] to the ionization potential of the metal cation M. On the other hand, chalcogenides[20] (X=S,Se) can be made out of Q^4 and Q^2 species only [which leads to a shift of (1) to the right] or, at least, of a mixture of all Q^n's which happens in systems with modifier cations of smaller sizes.[21] Noteworthy is the fact that global constraint counting[1] does not distinguish between the aforementioned systems, although the location of the rigidity and stress transitions should be obviously changed.

II. MODELING NON-MEAN-FIELD RIGIDITY

A. Classification of the interaction forces

Historically, the modeling of elastic properties of amorphous solids has been mostly based on the imposition of distance constraints to replace bonding forces[1,2] between atoms. In this constraint approach, the restriction to the interaction of only nearest-neighbor bond-bending and bond-stretching forces deserves some comments with respect to simulated glass structures and experiment.

In toy models of glasses[2] with vibrational Hamiltonians, the mean coordination change is achieved by a (random or selective) removal of bonds between atoms of the network. This implicitely assumes that interactions between nonconnected atoms are forced to be exactly zero. Furthermore, even for connected atoms, dihedral interactions or even more weaker forces (van der Waals, hydrogen) are not taken into account (see, however, Ref. 22). By imposing constraints on the strongest interactions only, it is implicitly assumed that higher-frequency motions are quenched and one expects that rigid structures have no vibrational modes on long (experimental) time scales. The separation into strong and weak forces is therefore central in the constraint approach and becomes meaningful when the difference between the strong and weak interactions display a significant gap. The neglected weaker forces have an experimental signature from inelastic neutron scattering, however.[23] Studies on the vibrational density of states show that the floppy mode energy supposed to be zero in the toy models has a finite value, i.e., it is blueshifted, forming a peak at around 4 meV in a Ge-As-Se system, although the frequency of the peak remains constant for mean coordination numbers up to $\bar{r}=2.4$. The area of the peak obtained from a deconvolution gives a spectral weight that is exactly equal to the floppy mode fraction f. In pure selenium, this spectral weight is close to 1/3, a value that one would expect simply from a constraint counting based on nearest-neighbor interactions. The shortcoming of the approach is therefore revealed in the shift from zero to a finite frequency of f but, as the area of the peak does not depend on the network mean coordination number, one can assume that the neglect of residual forces will only introduce a constant drift in the constraint counting. Application of constraint counting over the years have shown that it can predict precisely the location of elastic thresholds for very different systems,[3,4,13,16] oxides or chalcogenides, network or binary conducting glasses.

The nonobservation[24] of the predicted increase in elastic constants as a power law[2] with composition in the rigid phase from ultrasonic data has been another stressed limitation of the constraint approach even though it has been shown that this was mostly resulting from the weak excitation laser power.[25] At low laser excitation, Brillouin scattering measurements on sodium silicates[13] finally showed the anticipated power-law variation for the longitudinal and transverse acoustic modes, in harmony with the constraint approach. It suggests that in oxide glasses nearest-neighbor forces far exceed the more-distant-neighbor interactions in contrast with lone-pair-bearing chalcogenides.

A natural question emerging from a theoretical viewpoint would be in this case how accurately force-field molecular dynamics or tight-binding methods can describe the onset of rigidity in glasses by taking into account more distant interactions. Although the structure and physical properties of stoichiometric chalcogenides have been studied with approximate *ab initio* methods[26] or density-functional-based tight-binding methods,[27] glasses with changing composition using these tools have been considered only very recently[28] but not in the present context. On the other hand, classical molecular dynamics simulations using a Born-Mayer-Huggins-like potential have been able to show onset of rigidity under pressure in silica and germania[29,30] with low-frequency modes appearing in the vibrational densities of states in low-pressurized glasses. Compositionally driven rigidity transitions using *ab initio* fitted force-field models[31] have been considered only very recently. Although two- and three-body interatomic interactions are considered, the calculated mechanical behavior is optimized[32] at the mean coordination number $\bar{r}=2.4$.

The latter results suggest that bond distance constraints capture a large part of the picture. They certainly do not one allow one to have a full description of the structural or physical properties as would be obtained from simulations using force-field methods, but they succeed in predicting accurately the *location* of the transitions. However, one has to keep in mind that the vibrational and mechanical properties cannot be fully described using these methods. In the following, we therefore concentrate only on the location of the two transitions defining the intermediate phase.

B. Cluster construction

To describe non-mean-field rigidity, size-increasing cluster approximations (SICAs) can be used to infer the effect of the speciation on the location and the width of the intermediate phase. These methods were first introduced to study the medium-range order of amorphous insulators[33] and the growth of fullerenes.[34] They have been used in the context of floppy to rigid transitions for group IV chalcogenides.[8]

We consider a network of large N with tetrahedra Q^4, Q^3, and Q^2 having respective probabilities $p_4^{(l=1)}$, $p_3^{(1)}$, and $p_2^{(1)}$. The behavior of the $p_i^{(1)}$'s with modifier concentration x can be determined from the normalization condition

$$p_4^{(1)}+p_3^{(1)}+p_2^{(1)}=1, \tag{3}$$

a charge conservation law

$$R=\frac{2x}{1-x}=p_3^{(1)}+2p_2^{(1)}, \tag{4}$$

and the definition of the equilibrium constant[18] of the reaction (1). With these equations, the speciation is fully determined with respect to x (or R) and given by

$$p_3^{(1)}=\frac{R(2-R)}{1+\sqrt{(1-R)^2+4K_eR(2-R)}} \tag{5}$$

out of which is obtained $p_2^{(1)}=(R-p_3^{(1)})/2$ and $p_4^{(1)}=1-p_3^{(1)}-p_2^{(1)}$.

Starting from this short-range-order distribution $p_i^{(1)}$ (the basic SICA unit at $l=1$), one constructs the 12 possible structural corner- (6) and edge-sharing (6) arrangements of two basic units ($l=2$), i.e., Q^4-Q^4, Q^4-Q^3, Q^4-Q^2, Q^3-Q^3, etc. Three energy gains E_{stress}, E_{iso}, and E_{flex} are defined following the mechanical nature of the created cluster (stressed rigid, isostatically rigid, and flexible). Edge-sharing tetrahedra (EST) involve an energy gain E_{ES}. The probabilities of the created clusters ($l=2$) are given by

$$p_{kj}^{(2)}=\frac{W_{kj}}{\mathcal{Z}}p_k^{(1)}p_j^{(1)}\exp(-E_i/k_BT) \tag{6}$$

with $i=stress$, iso, $flex$, or ES. W_{kj} is a statistical factor taking into account the number of equivalent ways to connect two ($l=1$) units together.[35] $\mathcal{Z}$ normalized the step-l probabilities to 1.

Constraint counting is then applied on each of the ($l=2$) clusters and this leads to the number of floppy modes[2] of the network given by

$$f^{(2)}=3-n_c^{(2)}=3-\frac{\sum_{k,j}n_{c(kj)}p_{kj}^{(2)}}{\sum_{k,j}N_{kj}p_{kj}^{(2)}}, \tag{7}$$

where N_{kj} and $n_{c(kj)}$ are, respectively, the number of atoms and the number of constraints, arising from bond-bending and bond-stretching forces, of the cluster with probability $p_{kj}^{(2)}$. For an r-folded atom, the number of bond-stretching and bond-bending mechanical constraints is, respectively, $r/2$ and $(2r-3)$. Because of extra constraints, ring structures have to be counted following a different scheme.[2,8] Using these counting algorithms, one is then able to evaluate the mechanical nature of the created cluster ($n_c^{(l)}>0$ or $n_c^{(l)}<0$ or $n_c^{(l)}=0$) and this defines the energies E_i. For instance, on this basis Q^4-Q^4 connections are stressed rigid ($n_c=3.67$) whereas Q^4-Q^3 connections are isostatically rigid (stress-free).

Once this is set and starting from a flexible network where stressed rigid dendritic Q^4-Q^4 connections are absent and decreasing x, one can investigate at what concentration $x_{c(1)}$ the network will have a vanishing of $f^{(2)}$ (rigidity transition) according to Eq. (7), and at what concentration $x_{c(2)}$ the network will not be able to avoid any more dendritic stressed rigidity. Here stressed rigidity is achieved by corner-sharing Q^4's. This point in composition is the stress transition. The whole calculation is performed for a given amount of medium-range order characterized by the fraction η of edge-sharing tetrahedra in the base glass because η can be simply related[8] to the Boltzmann factor $e_{ES}=\exp(-E_{ES}/k_BT)$ in the basic network-forming limit ($x=0$, $p_4^{(1)}=1$).

III. RESULTS

With the construction established, one can now investigate how the mechanical nature of the network changes with modifier concentration, for various equilibrium constants K_e and edge-sharing fractions η.

A. Width of the intermediate phase

Figure 2 shows the location of the transitions. Large equilibrium constants K_e (corresponding to a Q^2-rich glass) will induce a large width for the IP. However, one observes that K_e mostly affects the location $x_{c(2)}$ of the stress transition whereas the location of the rigidity transition $x_{c(1)}$ remains almost constant. Noteworthy is also the shift from the mean-field (MF) rigidity transition at $x_c=0.20$ to lower x that arises from the presence of weakly stressed Q^4 EST ($n_c=3.33$ per atom, due to the ring correction[2,8]). With a weaker rigidity due to the presence of the latter, part of the strain is captured in the EST, and onset of flexibility can happen at lower modifier concentration x. As for IV-VI network glasses,[8] the

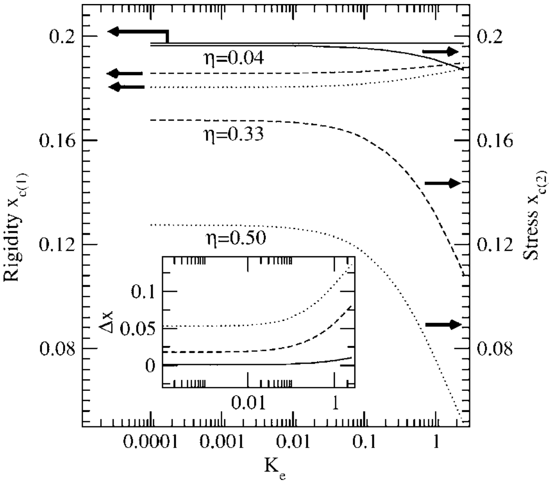

FIG. 2. Location of the rigidity $x_{c(1)}$ and the stress transition $x_{c(2)}$ (right axis) as a function of the equilibrium constant K_e for three fractions η of edge-sharing tetrahedra in the base glass ($\eta=0.04$, solid line; $\eta=0.33$, broken line; $\eta=0.50$, dotted line). With increasing η and K_e, the width $\Delta x = x_{c(1)} - x_{c(2)}$ becomes larger, as seen from the inset.

width $\Delta x = x_{c(2)} - x_{c(1)}$ of the IP increases with the fraction η of EST due to the shift of the location of the stress transition (Fig. 2). The change in speciation from a Q^3-rich to a Q^2-rich glass contributes, however, to an additional broadening of the IP.

The trend with K_e observed in Fig. 2 can be further characterized from the computation of the probability of stressed rigid and isostatically rigid clusters (Fig. 3). When the reaction (1) is shifted to the left side (low K_e, i.e., a Q^3-rich glass), each modifier molecule will create mostly two flexible Q^3 units ($n_c=2.55$ per atom) which serve to accumulate isostatically rigid subregions of the network, as Q^4-Q^3 connections ($n_{c(43)}/N_{43}=3$) are likely to appear. These are maximum at the stress transition (solid line, Fig. 3), consistently with numerical simulations.[6] On the other hand, a higher value of K_e leads to the growth of even more flexible units (Q^2's, $n_c=2.0$ per atom) at the expense of Q^3's, and will produce a stress transition at lower x (broken line, Fig. 3). Indeed, increasing K_e at fixed x decreases the network mean coordination number and favors flexible Q^4-Q^2 instead of isostatically rigid Q^4-Q^3 bondings. As a result, with growing concentration x, the network will lose stress earlier and will display a lower isostaticity in the IP. Thus $x_{c(2)}$ is shifted to lower x. One should finally note that within this model the rigidity transition is not directly observable from the structural cluster probabilities, whereas it has a clear signature in free energy (see below). Experimentally, both transitions are detected from calorimetric measurements[3,4] while structural correlations in diffraction[36] acknowledge only the stress transition at $x_{c(2)}$.

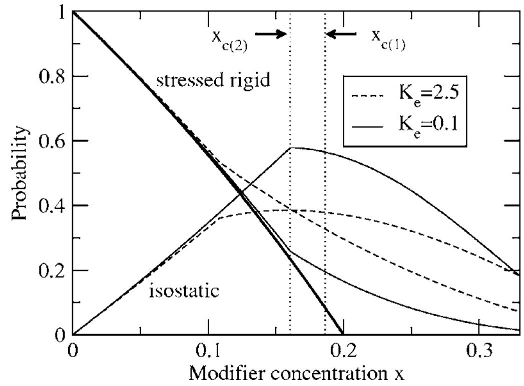

FIG. 3. Probability of finding stressed rigid and isostatically rigid clusters with respect to the modifier concentration x for two different equilibrium constants: $K_e=0.1$ (solid line) and 2.5 (broken line). Note that the stressed rigid cluster probability extrapolates to $x_c=0.20$ in the MF description (thick line). The dotted vertical lines serve to define the two transitions and the intermediate phase for $K_e=0.1$. Here $\eta=0.33$.

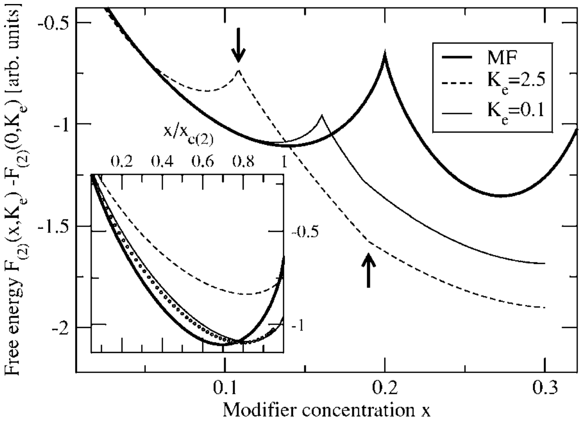

FIG. 4. Free energy $\mathcal{F}_{(2)}(x,K_e) - \mathcal{F}_{(2)}(0,K_e)$ of the system as a function of the modifier concentration x in the mean-field case (thick solid line), and for two different equilibrium constants $K_e=0.1$ (solid, line) and 2.5 (broken line), both for $\eta=0.33$. The arrows indicate the stress and rigidity transitions for $K_e=2.5$. The inset shows the same quantity with x rescaled to its stress transition composition $x_{c(2)}$, together with the free energy (dots) minimized by K_e. In all, $k_BT=1$.

B. Constraint free energy

The constraint-related free energy is now considered, following the approach initially reported by Naumis.[37] The free energy of the system is given by

$$\mathcal{F}_{(2)}(x,K_e) = -f^{(2)} + k_BT\sum_{k,j} p_{kj}^{(2)} \ln p_{kj}^{(2)}, \tag{8}$$

where $-f^{(2)}$ is the stress energy equal to the number of redundant constraints, i.e., additional constraints that cannot be balanced by the degrees of freedom, and which vanish for $x > x_{c(1)}$.

Figure 4 shows that the stress transition at $x = x_{c(2)}$ is first order for any K_e. However, with respect to the mean-field case (thick solid line) where $x_{c(1)} = x_{c(2)}$, the jump of the first derivative $\partial\mathcal{F}_{(2)}(x,K_e)/\partial x$ at $x = x_{c(2)}$ decreases with growing K_e. In the MF case, this jump is equal to 75.2±0.5, whereas it is only 45.3±0.3 for $K_e=2.5$. This suggests that the transition broadens when the equilibrium (1) shifts to the right, leading to a Q^2-rich glass. On the other hand, the change in character of the rigidity transition with K_e is weak and second order. Finally, some chemical self-organization of the network is allowed through an adaptative speciation. As stress costs energy, it is natural to imagine that the glass network will try to self-organize in the stressed rigid phase to decrease the energy by rewiring and reset some weaker bonds such as the ionic M-X ones that will lead to a Q^n species recombination. In the present description, this means that at a given concentration $x < x_{c(2)}$, the minimization of the free energy can be accomplished with respect to K_e. The equilibrium constant K_e minimizing $\mathcal{F}(x, K_e)$ provides then an estimation of the speciation via Eq. (5).

This leads to a stress transition at $x = x_{c(2)} = 0.17$ and a free energy (dots in the inset of Fig. 4) that is very close to the $K_e = 0.1$ speciation model and to sodium silicates.[19]

IV. SUMMARY AND CONCLUSIONS

In summary, there are different ways for a flexible system to self-organize in order to avoid stress, either by nucleating weakly stressed edge-sharing tetrahedra such as in network glasses ($\mathrm{Ge}_x\mathrm{Se}_{1-x}$) or by producing also more flexible species (Q^2's) in multicomponent systems, that serve to balance the addition of new constraints. Both delay the onset of stressed rigidity. As a conclusion, we provide a prediction of the IP for sodium seleniosilicates ($M = \mathrm{Na}$, $X = \mathrm{Se}$) that have an EST fraction of $\eta = 0.50$ in the base network former SiSe_2,[38] and an equilibrium constant $K_e = 0.15$.[20] According to the present approach, one therefore expects a stress transition at $x_{c(2)} = 0.11$, a rigidity transition at $x_{c(1)} = 0.18$, and a width for the intermediate phase of about $\Delta x = 0.07$. Larger structural correlations ($l > 2$) will probably refine this picture and are under consideration.

ACKNOWLEDGMENTS

It is a pleasure to acknowledge ongoing discussions with P. Boolchand, B. Goodman, J. C. Phillips, and M. Malki during the course of this work. Thank you to L. Pricoupenko and R. Chitra for a careful review of the revised manuscript, and to J. C. Mauro for signaling Ref. 32.

---

[1] J. C. Phillips, J. Non-Cryst. Solids **34**, 153 (1979).
[2] M. F. Thorpe, J. Non-Cryst. Solids **57**, 355 (1983).
[3] D. Selvanathan, W. Bresser, and P. Boolchand, Phys. Rev. B **61**, 15061 (2000).
[4] S. Chakravarty, D. G. Georgiev, P. Boolchand, and M. Micoulaut, J. Phys.: Condens. Matter **17**, L7 (2005).
[5] F. Wang, S. Mamedov, P. Boolchand, B. Goodman, and M. Chandrasekhar, Phys. Rev. B **71**, 174201 (2005).
[6] M. F. Thorpe, D. J. Jacobs, M. V. Chubynsky, and J. C. Phillips, J. Non-Cryst. Solids **266-269**, 859 (2000).
[7] M. V. Chubynsky, M. A. Briere, and N. Mousseau, Phys. Rev. E **74**, 016116 (2006).
[8] M. Micoulaut and J. C. Phillips, Phys. Rev. B **67**, 104204 (2003).
[9] J. Barre, A. R. Bishop, T. Lookman, and A. Saxena, Phys. Rev. Lett. **94**, 208701 (2005).
[10] A. J. Rader, B. Hespenheide, L. Kuhn, and M. F. Thorpe, Proc. Natl. Acad. Sci. U.S.A. **99**, 3540 (2002).
[11] J. C. Phillips, Phys. Rev. Lett. **88**, 216401 (2002).
[12] R. Monasson, R. Zecchina, S. Kirkpatrick, B. Selman, and L. Troyansky, Nature (London) **400**, 133 (1999).
[13] Y. Vaills, T. Qu, M. Micoulaut, F. Chaimbault, and P. Boolchand, J. Phys.: Condens. Matter **17**, 4889 (2005).
[14] For a review, see B. O. Mysen and P. Richet, *Silicate Glasses and Melts: Properties and Structure* (Elsevier, Amsterdam, 2005).
[15] B. O. Mysen, Eur. J. Mineral. **15**, 781 (2003).
[16] M. Zhang and P. Boolchand, Science **266**, 1355 (1994).
[17] J. F. Stebbins, Nature (London) **330**, 465 (1987).
[18] J. F. Stebbins, J. Non-Cryst. Solids **106**, 359 (1988).
[19] H. Maekawa and T. Yokokawa, Geochim. Cosmochim. Acta **61**, 2569 (1997).
[20] A. Pradel, G. Taillades, M. Ribes, and H. Eckert, J. Non-Cryst. Solids **188**, 75 (1995).
[21] C. M. Schramm, B. H. DeJong, and V. F. Parziale, J. Am. Chem. Soc. **106**, 4396 (1984).
[22] M. F. Thorpe and Y. Cai, J. Non-Cryst. Solids **114**, 19 (1989).
[23] W. A. Ramatikahara, R. L. Cappelletti, P. Boolchand, B. Halfpap, F. Gompf, D. A. Neumann, and H. Mutka, Phys. Rev. B **44**, 94 (1991).
[24] J. Y. Duquesne and G. Bellessa, J. Phys. Colloq. **46**, C10-445 (1986).
[25] J. Gump, I. Finkler, H. Xia, R. Sooryakumar, W. J. Bresser, and P. Boolchand, Phys. Rev. Lett. **92**, 245501 (2004).
[26] S. Blaineau, P. Jund, and D. A. Drabold, Phys. Rev. B **67**, 094204 (2002).
[27] S. I. Simdyankin, S. R. Elliott, Z. Hajnal, T. A. Niehaus, and Th. Frauenheim, Phys. Rev. B **69**, 144202 (2004).
[28] J. Li and D. A. Drabold, Phys. Rev. B **64**, 104206 (2001); D. N. Tafen, D. A. Drabold, and M. Mitkova, *ibid.* **72**, 054206 (2005).
[29] K. Trachenko and M. T. Dove, J. Phys.: Condens. Matter **14**, 1143 (2002).
[30] K. Trachenko, M. T. Dove, V. Brazhkin, and F. S. El'kin, Phys. Rev. Lett. **93**, 135502 (2004).
[31] J. C. Mauro and A. K. Varshneya, J. Am. Ceram. Soc. **89**, 2323 (2006).
[32] J. C. Mauro and A. K. Varshneya, J. Am. Ceram. Soc. (to be published).
[33] M. Micoulaut, R. Kerner, and D. M. dos Santos-Loff, J. Phys.: Condens. Matter **7**, 8035 (1995).
[34] R. Kerner, K. Penson, and K. H. Bennemann, Europhys. Lett. **19**, 363 (1992).
[35] For a corner-sharing tetrahedron, the statistical factor is $W_{kj} = (2 - \delta_{kj}) r_k r_j$ whereas for an edge-sharing tetrahedron it is $W_{kj} = 2(2 - \delta_{kj}) \binom{r_k}{2} \binom{r_j}{2}$. Here, r_i and r_k are the coordination numbers of the involved species and δ_{kj} is the Kronecker symbol.
[36] Y. Wang, E. Ohata, S. Hosokawa, M. Sakurai, and E. Matsubara, J. Non-Cryst. Solids **337**, 54 (2004).
[37] G. G. Naumis, Phys. Rev. B **61**, R9205 (2000).
[38] M. Tenhover, M. A. Hazle, and R. K. Grasselli, Phys. Rev. Lett. **51**, 404 (1983).